

Chemical and Electrochemical Generation of Superoxide Ion in 1-butyl-1-methylpyrrolidinium bis(trifluoromethylsulfonyl)imide

Maan Hayyan^{1,2,*}, Farouq S. Mjalli³, Inas M. AlNashef⁴, Mohd Ali Hashim^{1,2}

¹ University of Malaya Centre for Ionic Liquids (UMCiL), University of Malaya, 50603 Kuala Lumpur, Malaysia

² Department of Chemical Engineering, University of Malaya, 50603 Kuala Lumpur, Malaysia

³ Petroleum & Chemical Engineering Department, Sultan Qaboos University, Muscat 123, Oman

⁴ Chemical Engineering Department, King Saud University, Riyadh 11421, Saudi Arabia

*E-mail: maan_hayyan@yahoo.com

Received: 15 July 2012 / Accepted: 19 August 2012 / Published: 1 September 2012

Ionic liquids (ILs) are currently attracting the attention of both researchers and industry due to their fascinating properties in different applications such as extraction, purification, catalysis, separation and electrochemical applications. The generation of superoxide ion ($O_2^{\bullet-}$) in ILs is one of these interesting areas. In this work, $O_2^{\bullet-}$ was generated and analyzed electrochemically using cyclic voltammetry and chronoamperometry techniques from O_2 dissolved in 1-butyl-1-methylpyrrolidinium bis(trifluoromethylsulfonyl)imide [BMPyrr][TFSI]. Furthermore, $O_2^{\bullet-}$ was generated chemically by dissolving potassium superoxide in the same IL. UV/Vis spectrophotometry was used for testing the stability of the generated $O_2^{\bullet-}$. The results showed that $O_2^{\bullet-}$ was stable in this IL. This encourages further investigation on the use of this particular class of ILs in various applications involving the $O_2^{\bullet-}$. For our best knowledge this is the first time that [BMPyrr][TFSI] was used for the chemical generation of $O_2^{\bullet-}$.

Keywords: ionic liquids; superoxide ion; pyrrolidinium cation; bis(trifluoromethylsulfonyl)imide; cyclic voltammetry; chronoamperometry.

1. INTRODUCTION

$O_2^{\bullet-}$ that is generated by the one electron reduction of O_2 is one of the most interesting species among reactive oxygen species in biological processes [1-2]. $O_2^{\bullet-}$ is an anionic radical and it behaves either as an electron donor, an electron reducing agent, an oxidant, a base or as a nucleophile [3-5].

The superoxide term has prompted many researchers to presume an extraordinary degree of reactivity for $O_2^{\bullet-}$, especially as a strong oxidant and an initiator of radical reactions [6-7].

$O_2^{\bullet-}$ was considered to be a little more than an interesting chemical curiosity for many years due to its difficult stability for a long period. Sawyer and Roberts (1966) had started their interest in the reactivity of $O_2^{\bullet-}$ with the discoveries that electrochemical reduction of O_2 in dimethyl sulfoxide (DMSO) yielded a stable $O_2^{\bullet-}$ [8].

$O_2^{\bullet-}$ can be generated either chemically by solvation of KO_2 in aprotic solvents, or electrochemically *via* direct electrochemical reduction of O_2 in aprotic organic solvents, typically $E = -1.0$ V vs. SCE [9-11].

However, due to the limitations of using aprotic solvents in terms of their high volatility, low boiling points and the negative ecological effects, no industrial implementations of the $O_2^{\bullet-}$ have been adopted. Therefore, the use of ILs is more preferable for $O_2^{\bullet-}$ generation [12].

ILs have unique properties as compared with conventional solvents; they are nonvolatile, nonflammable, and have high ionic conductivity, high thermal stability, large electrochemical windows, and moderate dissolvability of organic compounds as well as adjustable miscibility and polarity. However, they have higher viscosity than traditional solvents, e.g. acetonitrile. This results in lower diffusion coefficients of the electroactive species than would be observed in conventional solvents [13-19].

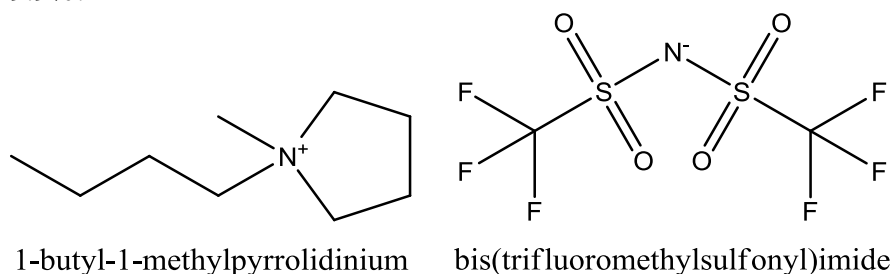
ILs are receiving wide recognition and special attention as successful and unique solvents for various reactions [20-24] and separation processes [25-29]. Currently, ILs are being investigated as promising electrolytes for applications of gas sensing [30-31], fuel and solar cells, organometallic synthesis, electrochemical devices, capacitors, lubricants, stationary phases for chromatography; matrices for mass spectrometry, supports for the immobilization of enzymes, in separation technologies, as liquid crystals, templates for synthesis of nano-materials and materials for tissue preservation, in the preparation of polymer-gel catalytic membranes, biphasic catalysis, and in the generation of high conductivity materials [32].

The novel feature of ILs, to be used as solvents, is the possibility of their design with the required properties for task specific applications [16]. ILs that are used in standard chemical processing unit operations can provide separations and reactions more efficiently, more reliability, faster, and more integrated compared to the conventional unit operations [33-34].

Many studies reported that the stability of the generated $O_2^{\bullet-}$ depends strongly on the type of the cation of the IL. For instance, Evans *et al.* (2004) and Hayyan *et al.* (2010, 2012) reported that $O_2^{\bullet-}$ reacted with quaternary phosphonium cations based ILs [35-37]. Other research groups [38-40] reported that $O_2^{\bullet-}$ was not stable in imidazolium-based ILs. Recently, AlNashef *et al.* (2010) found that $O_2^{\bullet-}$ reacted with the imidazolium cation to produce the corresponding 2-imidazolones [41]. Accordingly, although cyclic voltammetry (CV) may indicate short term stability of $O_2^{\bullet-}$ in ILs, it may not be an effective screening criterion for the long-term stability. Rather, bulk electrolysis and appropriate analytical techniques are required [36].

2. MATERIALS AND METHODS

The IL used in this work is 1-butyl-1-methylpyrrolidinium bis(trifluoromethylsulfonyl)imide [BMPyrr][TFSI]. The IL was supplied by Merck and was of synthesis grade. Scheme 1 shows the structures of the cation and anion that make up the IL used in this study. The chemical formula, molecular weight and melting point of the IL are listed in Table 1. Dimethyl sulfoxide (DMSO) was purchased from Fisher with a purity of 99.98% and potassium superoxide (KO_2) from Sigma Aldrich with a purity of 99.9%.



Scheme 1. Structures of ions comprising the IL

Table 1. The formula, molecular weight and melting point of [BMPyrr][TFSI].

Formula	M. Wt. (g/mol)	Melting Point ($^{\circ}\text{C}$)
$\text{C}_{11}\text{H}_{20}\text{F}_6\text{N}_2\text{O}_4\text{S}_2$	422.41	-6

2.1. Electrochemical generation of O_2^{\bullet} (short term stability)

CV tests were performed as the electrochemical analysis technique since this method is extremely powerful and is among the most widely practiced of all electrochemical methods [42]. The IL to be used was dried overnight in a vacuum oven at 50°C . It should be noted that the ILs were acidic without pre-treatment, and the pH was 4-6. The pH of ILs was measured using pH strips from Merck. A very small quantity of KO_2 was added to the acidic IL until its pH became 7 [11,36,43]. AlNashef *et al.* (2001) reported that O_2^{\bullet} was not stable in some ILs because of the acidity of these ILs [44]. Therefore, small additions of KO_2 can neutralize the acidic ILs without affecting the electrochemistry in these ILs [36,43].

The electrochemistry was performed using EG&G 263A potentiostat/galvanostat (PAR) controlled by computer and data acquisition software. CVs were conducted in a one compartment cell since the time of the experiment is relatively small to affect the ILs. The cell was a jacketed vessel (10 ml volume) with a Teflon cap including 4 holes for the three electrochemical electrodes and for the gas sparging tube.

Glassy carbon macro-electrode (BASi, 3 mm diam) was used as working electrode for CV. Platinum electrode was used as a counter electrode. To avoid contaminating the target IL from water in the reference electrode, the content of the reference electrode was separated by glass frit, a filtering

material, and for this reason the Ag/AgCl electrode purchased from BASi was used [25-26]. The macro-electrodes were polished using alumina solution (BASi) and sonicated in distilled water for 10 min prior to each experiment. This was done to ensure that there are no impurities on the surface of the working electrode.

All experiments were performed in a dry glove box under either an argon or helium atmosphere. Prior to O_2 generation, a background voltammogram was obtained after removal of O_2 . The O_2 removal was achieved by purging the IL with dry N_2 . This particular method is quite effective and also simple to be employed. Previous studies reported that purging a solution with an inert gas can reduce the partial pressure of O_2 above the solution, and as a consequence the solubility of dissolved O_2 in the solution decreases according to Henry's law [45-46].

O_2 was then bubbled into the tested IL for at least 30 min to ensure that equilibrium was achieved [30,44,47-48]. In order to confirm that the tested IL is saturated with O_2 , CVs at different time intervals were conducted and the final measurement was taken when the cathodic peak current of the CV was constant. Between consecutive CV runs, O_2 was bubbled briefly to refresh the system and to remove any concentration gradients. N_2 or O_2 sparging was discontinued during the CV runs. The chronoamperometry (CA) measurements were conducted inside a Faraday cage to avoid any interference. The value of the steady state background current was deducted from the value obtained after sparging with O_2 to provide the net steady state current. The net value of the current was then used in the calculations [11].

2.2 Calculation of diffusion coefficient, solubility and charge transfer coefficient for O_2

In this study, both CV using macro-electrode and CA using ultramicro-electrode techniques were utilized to determine the diffusion coefficients and solubility of O_2 in the studied ILs. The following four equations were used [11,42-44]:

$$i_p = (2.99 \times 10^5) \alpha^{0.5} A C_o D_o^{0.5} v^{0.5} \quad 1$$

$$i_{ss} = 4nFD_o C_o r_o \quad 2$$

$$\left| E_p - E_{p/2} \right| = \frac{1.857RT}{\alpha F} \quad 3$$

where:

i_p : the cathodic peak current of CV in A

α : the charge transfer coefficient

A : the surface area of the macro working electrode in cm^2

C_o : the bulk concentration of O_2 in mol/ml

D_o : the diffusion coefficient of O_2 in cm^2/s

v : the potential sweep rate in V/s

E_p : the peak potential for the cathodic current in V

$E_{p/2}$: the half-peak potential for the cathodic current in V

R : the universal gas constant in J/(mol.K)

T : the absolute temperature in K

F : Faraday's constant 96485 C/mol

k^0 : the standard heterogeneous rate constant in cm/s

i_{ss} : the steady-state current of CA in A

n : the number of electrons

r_o : the radius of ultramicro-electrode

The reduction peak potential vs. the log of the sweep rate from CV results was first plotted to give a straight line. The value of α was calculated *via* Eq 3. This was then used in Eq 1 to obtain a value for $C_o D_o^{1/2}$. CA experiments were then used to determine a value for $C_o D_o$ in Eq 2. This would give two equations in terms of C_o and D_o . These equations were solved simultaneously to provide the values of C_o and D_o .

2.3 Chemical generation of $O_2^{\bullet-}$ (long-term stability)

DMSO was dried overnight in a vacuum oven. KO_2 was kept in a sealed vial filled with molecular sieves. The chemical generation of $O_2^{\bullet-}$ was performed by dissolving KO_2 in DMSO while stirring with a magnetic stirrer [1,39]. Subsequently, a certain amount of IL was added to the generated $O_2^{\bullet-}$ in DMSO to investigate the stability of $O_2^{\bullet-}$ with time. A computer-controlled UV/Vis spectrophotometer (PerkinElmer-Lambda 35) was used to measure the absorption spectra of $O_2^{\bullet-}$ every 10 min for two hours. The reference solution of spectral measurements was DMSO or DMSO solution containing an appropriate amount of IL [36,43].

3. RESULTS AND DISCUSSION

3.1. Electrochemical generation of $O_2^{\bullet-}$ (short term stability)

Figure 1 shows both the forward reduction peak and the backward oxidation peak in the IL after sparging with O_2 . The presence of the backward peak confirms that the generated $O_2^{\bullet-}$ is stable within the time limits of the experiments. The negligible background CV in the presence of N_2 indicates that this IL is electrochemically stable within this range of potential. The potential of $O_2^{\bullet-}$ generation was \approx (-1 V). Similar results were obtained in ILs previously reported in the literature [11-12,37-38,44,47,49-52]. This potential is in accordance with that reported by Katayama and co-workers (2004) where they found that the potential of the redox peaks corresponding to $O_2/O_2^{\bullet-}$ was -1.2 V vs. Fc/Fc^+ . This was equal to that in trimethyl-*n*-hexylammonium bis(trifluoromethylsulfonyl)imide

[TMHAm][TFSI]. Thus, the acceptor number of [BMPyrr][TFSI] is also comparable to those of AcN and DMSO.

It is known that the redox potential of $O_2/O_2^{\bullet-}$ depends dominantly on the degree of solvation of $O_2^{\bullet-}$, assuming that the solvation energy of electrically neutral O_2 remains approximately constant for different media [9]. As $O_2^{\bullet-}$ has a negative charge, the degree of solvation of $O_2^{\bullet-}$ increases as the acceptor number of the medium increases. Thus, the redox potential of $O_2/O_2^{\bullet-}$ becomes more positive with an increase in the acceptor number of the medium. The acceptor numbers of H_2O , AcN, DMSO, and DMF are 54.8, 19.3, 19.3, and 16.0, respectively [53]. For ILs media, Katayama *et al.* (2004) concluded that the observed redox potential of $O_2/O_2^{\bullet-}$ [TMHAm][TFSI] was close to those in DMSO and AcN, and having almost the same acceptor number as AcN and DMSO [38].

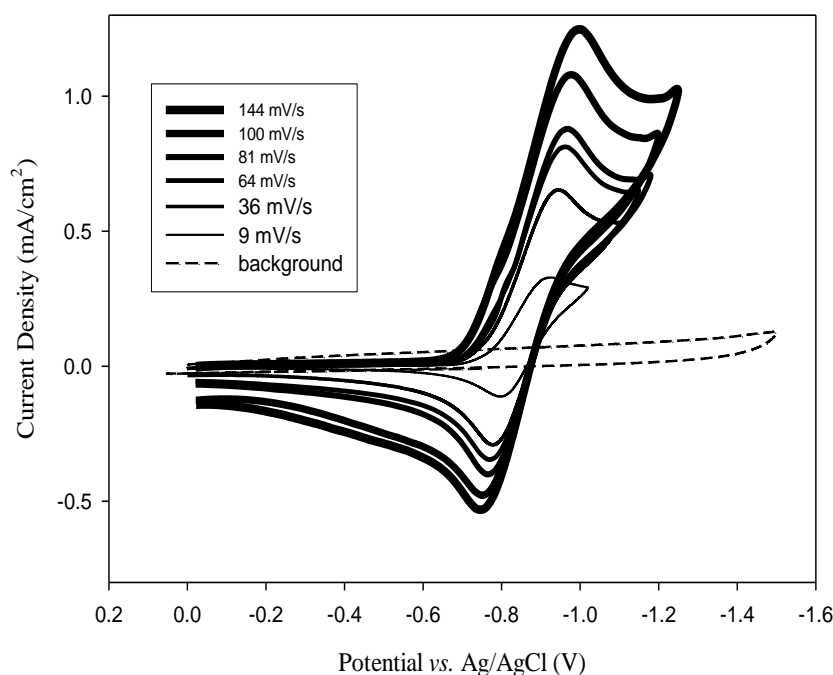


Figure 1. CVs in [BMPyrr][TFSI] after sparging with oxygen and nitrogen (background) at 25 °C and sweep rates of 9, 36, 64, 81, 100, 144 mV/s using GC macro-electrode.

Since charge compensating pyrrolidinium cations are in large excess and do not appear to form strong ion-pairs with the dianion, it is likely that the slow process is protonation of the highly basic dianion by trace H_2O within the IL medium. It is known that a protonation reaction will result in an anodic shift in reduction potential (from the reversible potential) of $59 \text{ mV}/\log[H^+]$. The near-equivalence of $E_{1/2}$ at 10.0 and 1.0 V/s supports the supposition that the protonation occurs from trace H_2O [54].

Randström *et al.* (2007) studied the influence of different binary and multi gases (air, Ar, N_2 , O_2) sparged in [BMPyrr][TFSI] on the cathodic stability. They observed the presence of a small peak within the voltage range of 0 to -1.55 V in all environments. They concluded that the presence of this peak was due to the presence of impurities in the studied IL [55], and when they tried to verify whether

this small peak was a characteristic of [BMPyrr][TFSI] or whether it belonged to impurities, they found that the small peak increased even in less pure sample, independent of the environment. It was clearly indicated that the origin of this peak was to be found in the presence of impurities or at least related to these impurities [55].

From the analysis of the CVs at various sweep rates, it was found that the net separation value between the cathodic peak E_p^c and half peak potential $E_{p/2}^c$, $|E_p^c - E_{p/2}^c|$, was not 56.5 mV, Table 2. Moreover, the difference between the reduction and oxidation peaks changes with sweep rate. This indicates that the electrochemical generation of $O_2^{\bullet -}$ in the studied ILs is not reversible. The peak currents and peak potentials are proportional to the square root and the log of the sweep rate, respectively. This is consistent with the electrochemistry of a kinetically irreversible soluble redox couple [42]. This is in agreement with the results reported for other ILs [11,44,56-57]. It should be noted that strong (bond forming) ion-pairing or protonation leads to electrochemical irreversibility [54,58-59].

Table 2. The net values of $|E_p^c - E_{p/2}^c|$ (mV) for sweep rate 9-144 mV/s at 25, 35 and 45 °C using GC macro-electrode.

Sweep rate (mV/s)	Temp. (°C)		
	25	35	45
144	152.3	171.1	178.8
100	141.5	142.1	143.8
81	122.9	128.4	140.2
64	122.0	130.5	130.9
63	112.4	117.5	119.8
9	104.2	105.8	119.1

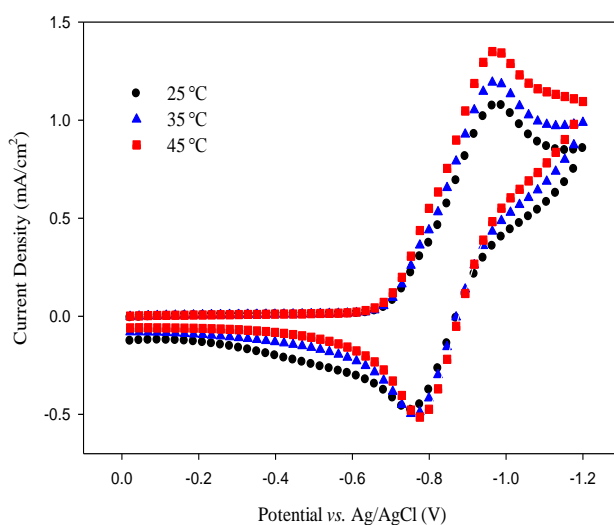


Figure 2. CVs in [BMPyrr][TFSI] after sparging O_2 as a function of temperature at 100 mV/s using GC macro-electrode.

Figure 2 shows that the reduction peak currents of CVs increase with temperature increase. This is due to the decrease of viscosity of the IL, and hence the increase in diffusion coefficients of O₂ in spite of the slight decrease of solubility of O₂. This is in agreement with other results reported previously [12,52].

The linear relationship between the reduction peak currents and the square root of sweep rates, Figure 3, indicates that the electrochemical reaction is diffusion controlled. This is in agreement with previous studies [12,54,60] and consistent with the electrochemistry of kinetically irreversible soluble redox couple [12,42,44].

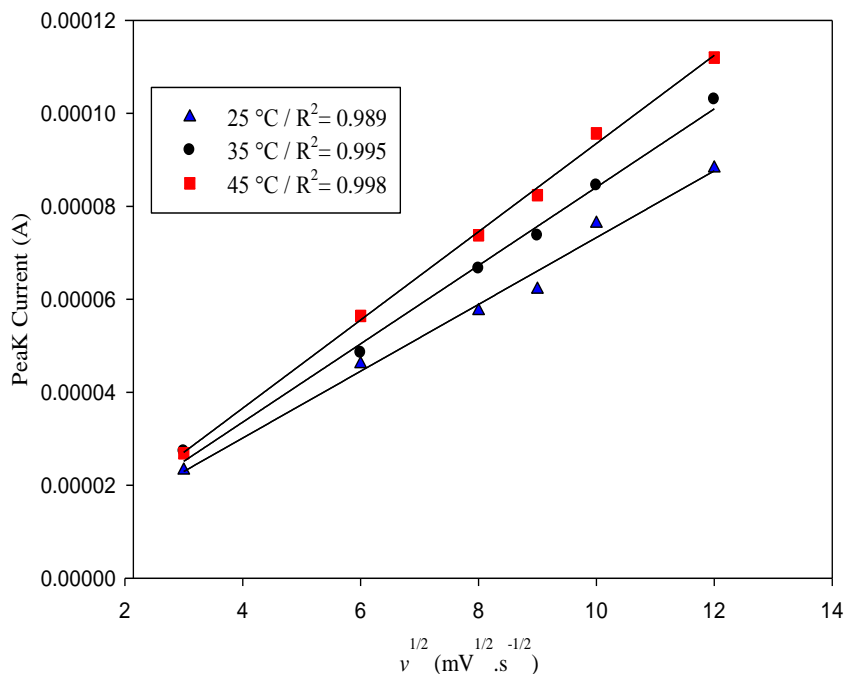


Figure 3. Currents of reduction peaks (O₂^{•-} generation) vs. square root of sweep rates $v^{1/2}$.

3.2. Calculation of the diffusion coefficient and solubility of O₂

Table 3 shows the numerical values of the diffusion coefficient and solubility of O₂ at different temperatures. It can be observed that the diffusion coefficients and CA steady state currents are increasing with increasing temperature while the solubility of O₂ is decreasing; this is in agreement with Katayama *et al.* (2005) and Hayyan *et al.* (2011, 2012) [11,43,50].

Table 3. Diffusion coefficients and solubility of O₂, CA steady state current, and charge transfer coefficient α in [BMPyrr][TFSI] at 25, 35 and 45 °C.

Temp. (°C)	Diffusion Coefficient $\times 10^{10}$ (m ² /s)	Solubility of O ₂ (mM)	Current (nA)	Charge Transfer Coefficient α
25	5.9	9.1	9.2	0.39
35	6.2	8.1	10.7	0.39
45	6.3	7.2	12.2	0.38

The diffusion coefficient and solubility of O_2 in [BMPyrr][TFSI] were different than the values determined by Katayama *et al.* (2005) as they reported a diffusion coefficient of $1.8 \cdot 10^{-10} \text{ m}^2/\text{s}$ and a solubility of 13.6 mM at 25°C . This difference can be attributed to the utilization of different equations, including Cottrell's equation and Eq 2, with gold working electrode as macro- and ultramicro- sizes. However, electrochemically speaking, this difference is acceptable since they have the same order of magnitude in comparison to the results reported herein, as shown in Table 3.

The values of diffusion coefficient of O_2 in [BMPyrr][TFSI] were in agreement with values reported by Evans *et al.* (2004) and Hayyan *et al.* (2011) [11,37].

Figure 4 shows that the steady state currents of CA increase with temperature increase, as stated in Table 3. Again, this is due to the reduction of the viscosity of the ILs with increasing temperature and consequently the increase of O_2 diffusivity. This is in agreement with that reported by Katayama research group (2005) where they used Au ultramicro-electrode ($10 \mu\text{m}$ diam.) to calculate the diffusion coefficients and solubility of O_2 in [BMPyrr][TFSI] [50].

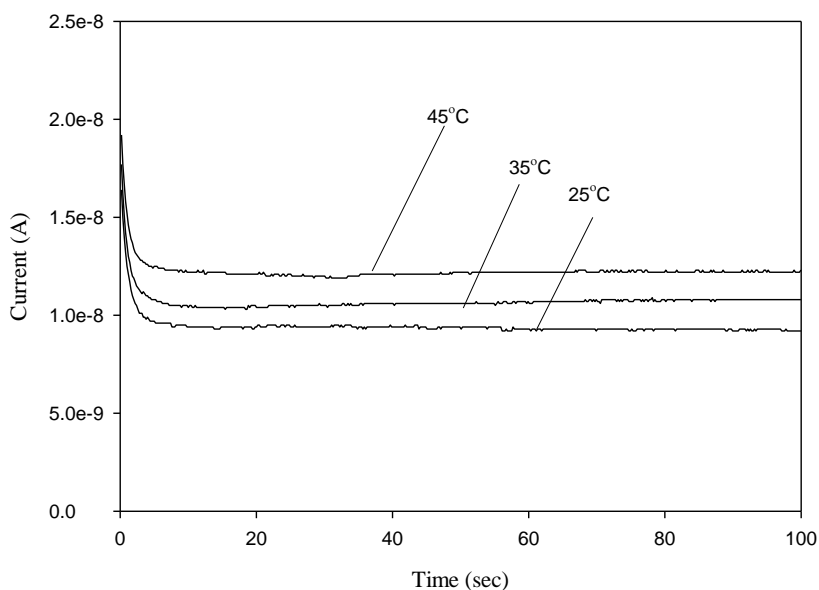


Figure 4. CAs of O_2 reduction in [BMPyrr][TFSI] at temperatures of 25°C , 35°C and 45°C using CF ultramicro-electrode.

3.3. Chemical generation of $O_2^{\bullet-}$ (long-term stability)

Figure 5 shows a slight decrease in absorbance peak of $O_2^{\bullet-}$ with time. This demonstrates that $O_2^{\bullet-}$ is very stable in this IL, and this confirms a high viability to serve as good media for the generation of a stable $O_2^{\bullet-}$.

Table 4 shows the rate constant of reaction, total consumption and consumption rate of $O_2^{\bullet-}$ in the studied IL. The rate constants were calculated based on the assumption of pseudo 1st order reaction between the cation of the ILs and $O_2^{\bullet-}$. The consumption rate of $O_2^{\bullet-}$ was calculated by dividing the concentration of $O_2^{\bullet-}$ being consumed over the time period of the measurement. The rate constant of

$O_2^{\bullet-}$ in [BMPyrr][TFSI] was estimated to be $2.6 \times 10^{-5} s^{-1}$. This value is similar in terms of the order of magnitude to that reported by AlNashef *et al.* (2010) and Hayyan *et al.* (2012) [36,41]. However, Table 4 illustrates that $O_2^{\bullet-}$ in [HMPyrr]⁺ has less consumption rate of $3.334 \times 10^{-3} mM/min$ and percentage of 13.28% in comparison to [BMPyrr]⁺ which has a consumption rate of $4.1 \times 10^{-3} mM/min$ and percentage of 17.9%. This confirms that $O_2^{\bullet-}$ is more stable with increasing the alkyl chain length attached to the cation of IL.

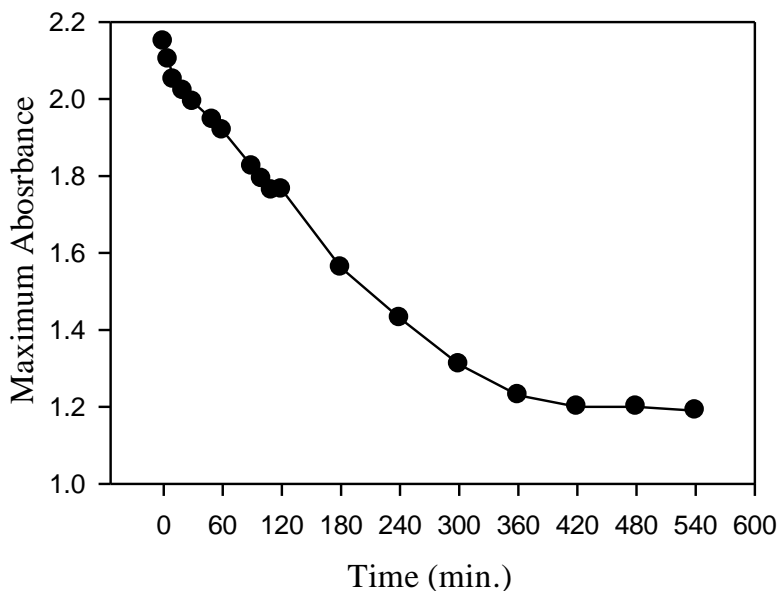


Figure 5. The change of superoxide absorbance peak with time in [BMPyrr][TFSI].

Table 4. Rate constant, total consumption percentage and consumption rate of $O_2^{\bullet-}$.

IL	Rate Constant $\times 10^5 (s^{-1})$	Total Consumption % of $O_2^{\bullet-}$ after 120 min	Consumption Rate of $O_2^{\bullet-} \times 10^3 (mM/min)$
[BMPyrr][TFSI]	2.6	17.90	4.100
[HMPyrr][TFSI]*	1.9	13.28	3.334

*[36]

4. CONCLUSIONS

$O_2^{\bullet-}$ was generated electrochemically using cyclic voltammetry (CV) and chronoamperometry (CA) techniques from O_2 dissolved in [BMPyrr][TFSI]. Furthermore, $O_2^{\bullet-}$ was generated chemically by the addition of KO_2 to the studied IL. A UV/Vis spectrophotometer was used for testing the long-term stability of generated $O_2^{\bullet-}$. The diffusion coefficients and solubility of O_2 were determined. It was found that diffusion coefficient of O_2 increased with temperature increase whereas the solubility decreased. The long-term stability of $O_2^{\bullet-}$ tests showed that $O_2^{\bullet-}$ in [BMPyrr][TFSI] is stable.

ACKNOWLEDGMENTS

The authors would like to express their thanks to the National Plan for Science, Technology, and Innovation at King Saud University (10-ENV1315-02), and to the University of Malaya HIR-MOHE (D000003-16001), University of Malaya Centre for Ionic Liquids (UMCiL), and to Sultan Qaboos University for their support to this research.

References

1. T. Oritani, N. Fukuhara, T. Okajima, F. Kitamura, T. Ohsaka, *Inorg. Chim. Acta*, 357 (2004) 436.
2. L. Packer, A.N. Glazer, *Methods in Enzymology*, Academic Press, New York, 1990.
3. I. Gülçin, Z. Huyut, M. Elmastas, H.Y. Aboul-Enein, *Arab. J. Chem.*, 3 (2010) 43.
4. A.A. Frimer, *The Chemistry of Functional Groups, Peroxides*, John Wiley & Sons Ltd, New York, 1983.
5. D.T. Sawyer, J.L. Roberts, *Acc. Chem. Res.*, 21 (1988) 469.
6. D.T. Sawyer, J.S. Valentine, *Acc. Chem. Res.*, 14 (1981) 393.
7. H. Xiao, H.-S. Hu, W.H.E. Schwarz, J. Li, *J. Phys. Chem. A*, 114 (2010) 8837.
8. D.T. Sawyer, J.L. Roberts Jr, *J. Electroanal. Chem.*, 12 (1966) 90.
9. D.T. Sawyer, *Oxygen chemistry*, Oxford University Press, USA, 1991.
10. D.T. Sawyer, A. Sobkowiak, J.L. Roberts, *Electrochemistry for Chemists*, Wiley, New York, 1995.
11. M. Hayyan, F.S. Mjalli, M.A. Hashim, I.M. AlNashef, X.M. Tan, *J. Electroanal. Chem.*, 657 (2011) 150.
12. M. Hayyan, F.S. Mjalli, I.M. AlNashef, M.A. Hashim, *J. Fluorine Chem.*, doi:10.1016/j.jfluchem.2012.06.028 (2012).
13. D.W. Armstrong, L. He, Y.S. Liu, *Anal. Chem.*, 71 (1999) 3873.
14. J.G. Huddleston, A.E. Visser, W.M. Reichert, H.D. Willauer, G.A. Broker, R.D. Rogers, *Green Chem.*, 3 (2001) 156.
15. J.G. Huddleston, R.D. Rogers, *Chem. Commun.*, (1998) 1765.
16. K.N. Marsh, J.A. Boxall, R. Lichtenthaler, *Fluid Phase Equilib.*, 219 (2004) 93.
17. C. Patrascu, F. Gauffre, F. Nallet, R. Bordes, J. Oberdisse, N. De Lauth-Viguerie, C. Mingotaud, *ChemPhysChem*, 7 (2006) 99.
18. H. Zhao, S. Xia, P. Ma, *J. Chem. Technol. Biotechnol.*, 80 (2005) 1089.
19. J. Liu, G. Jiang, Y. Chi, Y. Cai, Q. Zhou, J.T. Hu, *Anal. Chem.*, 75 (2003) 5870.
20. M.J. Earle, K.R. Seddon, *Pure Appl. Chem.*, 72 (2000) 1391.
21. S. Pandey, *Anal. Chim. Acta*, 556 (2006) 38.
22. C.P. Mehnert, R.A. Cook, N.C. Dispenziere, M. Afeworki, *J. Am. Chem. Soc.*, 124 (2002) 12932.
23. K. Popov, H. Rönkkömäki, M. Hannu-Kuure, T. Kuokkanen, M. Lajunen, A. Vendilo, P. Oksman, L.H.J. Lajunen, *J. Inclusion Phenom. Macrocyclic Chem.*, 59 (2007) 377.
24. D. Betz, P. Altmann, M. Cokoja, W.A. Herrmann, F.E. Kühn, *Coord. Chem. Rev.*, 255 (2011) 1518.
25. V.A. Cocalia, J.D. Holbrey, K.E. Gutowski, N.J. Bridges, R.D. Rogers, *Tsinghua Sci. Technol.*, 11 (2006) 188.
26. P. Vayssière, A. Chaumont, G. Wipff, *Phys. Chem. Chem. Phys.*, 7 (2005) 124.
27. A.E. Visser, R.P. Swatloski, W.M. Reichert, R. Mayton, S. Sheff, A. Wierzbicki, J.H. Davis, R.D. Rogers, *Environ. Sci. Technol.*, 36 (2002) 2523.
28. A.E. Visser, R.P. Swatloski, W.M. Reichert, S.T. Griffin, R.D. Rogers, *Ind. Eng. Chem. Res.*, 39 (2000) 3596.
29. P.-Y. Chen, C.L. Hussey, *Electrochim. Acta*, 50 (2005) 2533.
30. M.C. Buzzeo, C. Hardacre, R.G. Compton, *Anal. Chem.*, 76 (2004) 4583.

31. D.S. Silvester, K.R. Ward, L. Aldous, C. Hardacre, R.G. Compton, *J. Electroanal. Chem.*, 618 (2008) 53.
32. M. Hayyan, F.S. Mjalli, M.A. Hashim, I.M. AlNashef, *IJUM Eng. J.*, 12 (2011) 37.
33. H. Zhao, *Chem. Eng. Commun.*, 193 (2006) 1660.
34. H. Machida, R. Taguchi, Y. Sato, L. Florusse, C. Peters, R. Smith, *Front. Chem. Eng. China*, 3 (2009) 12.
35. M. Hayyan, F.S. Mjalli, M.A. Hashim, I.M. AlNashef, X.M. Tan, K.L. Chooi, *J. Applied Sci.*, 10 (2010) 1176.
36. M. Hayyan, F.S. Mjalli, M.A. Hashim, I.M. AlNashef, S.M. AlZahrani, K.L. Chooi, *J. Electroanal. Chem.*, 664 (2012) 26.
37. R.G. Evans, O.V. Klymenko, S.A. Saddoughi, C. Hardacre, R.G. Compton, *J. Phys. Chem. B*, 108 (2004) 7878.
38. Y. Katayama, H. Onodera, M. Yamagata, T. Miura, *J. Electrochem. Soc.*, 151 (2004) A59.
39. M.M. Islam, T. Imase, T. Okajima, M. Takahashi, Y. Niikura, N. Kawashima, Y. Nakamura, T. Ohsaka, *J. Phys. Chem. A*, 113 (2009) 912.
40. A. Rene, D. Hauchard, C. Lagrost, P. Hapiot, *J. Phys. Chem. B*, 113 (2009) 2826.
41. I.M. AlNashef, M.A. Hashim, F.S. Mjalli, M.Q. Ali, M. Hayyan, *Tetrahedron Lett.*, 51 (2010) 1976.
42. A.J. Bard, L.R. Faulkner, *Electrochemical Methods: Fundamentals and Applications*, Wiley, New York, 2001.
43. M. Hayyan, F.S. Mjalli, M.A. Hashim, I.M. AlNashef, S.M. Al-Zahrani, K.L. Chooi, *J. Mol. Liq.*, 167 (2012) 28.
44. I.M. AlNashef, M.L. Leonard, M.C. Kittle, M.A. Matthews, J.W. Weidner, *Electrochem. Solid State Lett.*, 4 (2001) D16.
45. M.E. Rollie, G. Patonay, I.M. Warner, *Ind. Eng. Chem. Res.*, 26 (1987) 1.
46. C. Zhao, A.M. Bond, R.G. Compton, A.M. O'Mahony, E.I. Rogers, *Anal. Chem.*, 82 (2010) 3856.
47. M.C. Buzzeo, O.V. Klymenko, J.D. Wadhawan, C. Hardacre, K.R. Seddon, R.G. Compton, *J. Phys. Chem. A*, 107 (2003) 8872.
48. K. Ding, *Portug. Electrochim. Acta*, 27 (2009) 165.
49. M.C. Buzzeo, O.V. Klymenko, J.D. Wadhawan, C. Hardacre, K.R. Seddon, R.G. Compton, *J. Phys. Chem. B*, 108 (2004) 3947.
50. Y. Katayama, K. Sekiguchi, M. Yamagata, T. Miura, *J. Electrochem. Soc.*, 152 (2005) E247.
51. D. Zigah, A. Wang, C. Lagrost, P. Hapiot, *J. Phys. Chem. B*, 113 (2009) 2019.
52. X.J. Huang, E.I. Rogers, C. Hardacre, R.G. Compton, *J. Phys. Chem. B*, 113 (2009) 8953.
53. V. Gutmann, *The Donor-Acceptor Approach to Molecular Interactions*, Plenum Press, New York, 1978.
54. S. O'Toole, S. Pentlavalli, A.P. Doherty, *J. Phys. Chem. B*, 111 (2007) 9281.
55. S. Randström, G.B. Appetecchi, C. Lagergren, A. Moreno, S. Passerini, *Electrochim. Acta*, 53 (2007) 1837.
56. M.T. Carter, C.L. Hussey, S.K.D. Strubinger, R.A. Osteryoung, *Inorg. Chem.*, 30 (1991) 1149.
57. I.M. AlNashef, M.L. Leonard, M.A. Matthews, J.W. Weidner, *Ind. Eng. Chem. Res.*, 41 (2002) 4475.
58. A. Demortier, A.J. Bard, *J. Am. Chem. Soc.*, 95 (1973) 3495.
59. J.-M. Savéant, *J. Phys. Chem. B*, 105 (2001) 8995.
60. D. Zhang, T. Okajima, F. Matsumoto, T. Ohsaka, *J. Electrochem. Soc.*, 151 (2004) D3.